JPE 16-6-6

http://dx.doi.org/10.6113/JPE.2016.16.6.2045
ISSN(Print): 1598-2092 / ISSN(Online): 2093-4718

Input Impedances of PWM DC-DC Converters: Unified Analysis and Application Example

Syam Kumar Pidaparthy* and Byungcho Choi†

*,†School of Electronics Engineering, Kyungpook National University, Daegu, Korea

Abstract

The input impedances of pulse width modulated (PWM) dc-to-dc converters, which dictate the outcomes of the dynamic interaction between dc-to-dc converters and their source subsystem, are analyzed in a general and unified manner. The input impedances of three basic PWM dc-to-dc converters are derived with both voltage mode control and current mode control. This paper presents the analytical expressions of the 24 input impedances of three basic PWM dc-to-dc converters with the two different control schemes in a factorized time-constant form. It also provides a comprehensive reference for future dynamic interaction analyses requiring knowledge of the converters' input impedances. The theoretical predictions of the paper are all supported by measurements on prototype dc-to-dc converters. The use of the presented results is demonstrated via a practical application example, which analyzes the small-signal dynamics of an input-filter coupled current-mode controlled buck converter. This elucidates the theoretical background for the previously-reported eccentric behavior of the converter.

Key words: Current mode control, Dynamic interaction, Input impedances, Middlebrook's extra element theorem, Middlebrook's feedback theorem, Pulse width modulated dc-to-dc converters, Voltage mode control

I. INTRODUCTION

When a pulse width modulated (PWM) dc-to-dc converter is powered by a nonideal source subsystem, its performance is significantly affected by the dynamic interaction between the dc-to-dc converter and the source subsystem. Because the outcomes of the dynamic interaction are dictated by the input impedances of the dc-to-dc converter [1]-[7], knowledge of the converter's input impedances is critically needed for the interaction analysis.

The input impedances of PWM dc-to-dc converters have been investigated by many researchers. However, the input impedances had long been treated as a subordinate subject in papers covering the dynamic interactions between the source subsystem and the converter downstream [3]-[7]. Even in papers dealing with the input impedances themselves [8], [9], the analyses were done case by case. Thus, they provide only limited information about their complex behavior.

In 2006, a paper was published [10] that provided fairly comprehensive information about the input impedances of the PWM converters. However, the paper only dealt with the PWM converters loaded with a pure resistor. The load of practical dc-to-dc converters is not a resistor but a complex combination of electronic devices, apparatus, and even power converters downstream. Accordingly, the results of the previous paper are not applicable in practice despite its theoretical value.

Recently, a new design and analysis method for the converters coupled with practical non-resistive loads has been reported [11], [12]. The proposed approach initially considers dc-to-dc converters loaded with an ideal current sink. The impacts of an actual load are later incorporated to predict the performance of the converter in the presence of actual load.

The source subsystem interaction can be analyzed in the same way as above. First the input impedances of a converter loaded with a current sink load are analysed. Then the effects of the source subsystem are evaluated. Finally, the impacts of the actual load are incorporated. In this approach, information about the input impedances of converters coupled with an ideal current sink is critically need. Accordingly, this paper presents new results on the input impedances of dc-to-dc converters coupled with a current sink load. The outcomes of this paper can be generally applied to the dc-to-dc

Manuscript received May 12, 2016; accepted Aug. 12, 2016
Recommended for publication by Associate Editor Yan Xing.
†Corresponding Author: bchoi@ee.knu.ac.kr
Tel: +82-53-950-6603, Fax: +82-53-950-5505, Kyungpook Nat'l Univ.
*School of Electronics Eng., Kyungpook National University, Korea

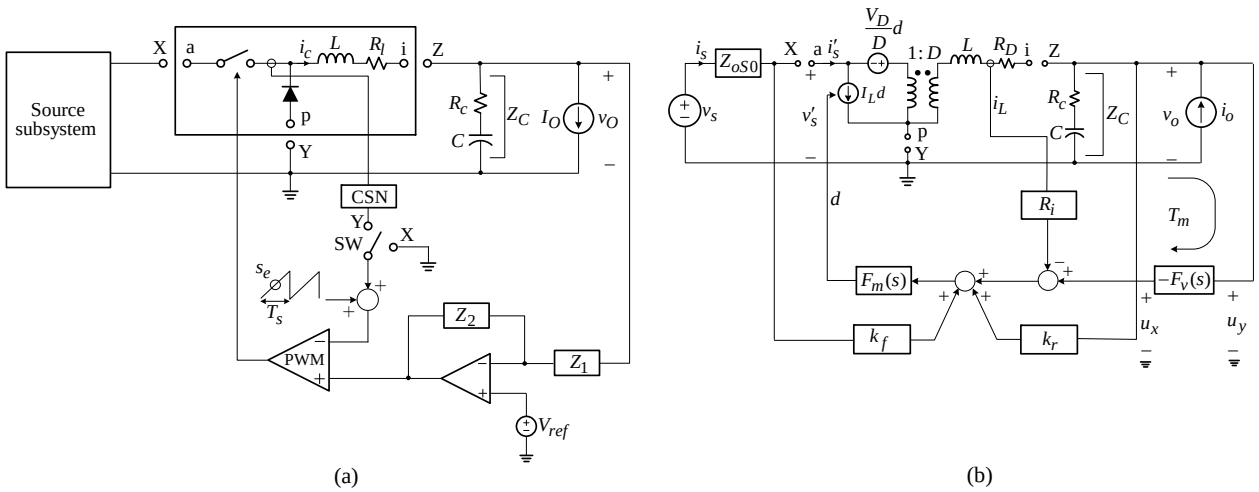

Fig. 1. PWM dc-to-dc converter combined with source subsystem. (a) General functional diagram for three basic PWM converters with voltage mode control or current mode control. The CSN represents the current sensing network and PWM is the pulsewidth modulation block. (b) Small-signal model.

converters coupled with practical loads.

As will be clarified in the forthcoming discussions, four different input impedances, each defined with a specific operational condition for the dc-to-dc converter, are involved in the dynamic interaction with the source subsystem. Thus, knowledge of these four impedances is required to fully analyze the dynamic interactions. The characteristics of these four impedances strongly depend on both the control method and the converter topology. The purpose of this paper is to propose a unified impedance analysis method, and to present expressions for the input impedances of PWM converters derived from the proposed analysis method.

Three basic PWM converters, the buck converter, boost converter, and buck/boost converter, are covered in this paper. The two most common control methods for PWM converters, the voltage mode control and current mode control, are considered. The impedances of the three types of PWM converters with the two different control schemes are all derived in a general and unified manner. The input impedances are initially derived using Middlebrook's extra element theorem [13] and the feedback theorem [14]. The resulting input impedances are then simplified into asymptotic expressions through the graphical Bode plot technique [15]-[17].

For the final outcome of the analysis, 24 input impedances of the three basic PWM converters with the two different control schemes are expressed in a factorized time-constant form, and later converted into Bode plots for general use in future dynamic interaction analyses involving dc-to-dc converters. The validity of the analysis method and the accuracy of the input impedances are supported by both computer simulations and experimental results.

An application example is given in Section V in order to demonstrate the use of the presented results. Section V deals with the small-signal analysis of the current-mode controlled buck converter coupled with an input filter in the front. This example clearly shows how knowledge about input impedances is used to comprehend the peculiar behavior of the converter, which has long been a subject of disputes and clarifications [4], [5].

II. Input Impedances of a PWM Converter

Fig. 1(a) shows a general functional diagram of the PWM converter combined with a practical source subsystem. The diagram represents a buck converter with connections {a-X p-Y i-Z}, a boost converter with {i-X a-Y p-Z}, and a buck/boost converter with {a-X i-Y p-Z}. The switch SW is at position X for the voltage mode control, and at position Y for the current mode control. The output port of Fig. 1(a) is terminated with an ideal current sink load, rather than a particular load subsystem. This makes it possible to perform an input impedance analysis based solely on only the dc output current, without any prior information on the load impedance characteristics [18].

Fig. 1 (b) is the small-signal model of Fig. 1(a), obtained by merging the unified model of the current mode control [19] into the PWM switch model [20] of the power stage circuit. The small-signal parameters shown in Fig. 1(b) are as follows: D is the duty ratio. $R_D = R_l + DD'R_e$ and $V_D = V_{ap} + (D-D')R_eI_L$, where $D' = 1-D$, and $R_e = 0$ for the buck converter; $R_e = R_c$ for the boost and buck/boost converters. $I_L = V_O / R_{DC}$ for the buck converter, $I_L = -V_O / (R_{DC}D')$ for the boost converter, and $I_L = V_O / (R_{DC}D')$ for the buck/boost converter, where $R_{DC} = V_O / I_O$. R_i represents the CSN gain. $F_m(s) = F_m' / (1 + s/\omega_p)$ is the transfer function of the PWM

TABLE I
PERFORMANCE CRITERIA FOR PWM CONVERTER WITH SOURCE SUBSYSTEM

$A_u = A_{uC}\dfrac{1}{1+\dfrac{Z_{oS0}}{Z_{iC}}}$	$Z_o = Z_{oC}\dfrac{1+\dfrac{Z_{oS0}}{Z_i'}}{1+\dfrac{Z_{oS0}}{Z_{iC}}}$	$T_m = T_{mC}\dfrac{1+\dfrac{Z_{oS0}}{Z_i''}}{1+\dfrac{Z_{oS0}}{Z_i'''}}$	$Z_i = Z_{iS\infty}\dfrac{1+\dfrac{Z_{oS0}}{Z_{iC}}}{1+\dfrac{Z_{oS\infty}}{Z_{iC}}}$

Transfer functions of dc-to-dc converter	**Transfer functions of source subsystem**
A_{uC}: closed-loop input-to-output transfer function	$Z_{iS\infty}$: input impedance with output port opened
Z_{oC}: closed-loop output impedance	Z_{oS0}: output impedance with input port shorted
T_{mC}: loop gain	$Z_{oS\infty}$: output impedance with input port opened
Z_{iC}: closed-loop input impedance	
Z_i': open-loop input impedance with output port shorted	
Z_i'': closed-loop input impedance with output voltage nullified	
Z_i''': open-loop input impedance	

block [19]: $F_m' = 1/((0.5s_n - 0.5s_f + s_e)T_s)$, and $\omega_p = \omega_s^2/(4F_m'(s_n + s_f))$ for all three converters, where s_n: the on-time slope of the sensed inductor current, s_f: the off-time slope of the sensed inductor current, s_e: the slope of the compensation ramp, and $\omega_s = 2\pi/T_s$ is the switching period. For the voltage mode control, $R_i = s_n = s_f = 0$. In addition, k_r/k_f represents the feedback/feedforward gain of the current mode control [19]: $k_r = -g_r DD'T_s R_i/(2L)$, and $k_f = -g_f DD'T_s R_i/(2L)$, where $g_r = 0$, and $g_f = 1$ for the buck converter; $g_r = 1$, and $g_f = 0$ for the boost converter; and $g_r = g_f = 1$ for the buck/boost converter. $F_v(s) = Z_2/Z_1$ is the voltage feedback compensation. In Fig. 1(b), the source subsystem is modeled in Thevenin's equivalent form, consisting of a small-signal voltage source v_s and an output impedance Z_{oS0}. The source subsystem can represent any of the practical voltage sources, ranging from standalone dc sources with passive filters to ac-dc converters with power factor correction.

The performance criteria for a dc-to-dc converter combined with a source subsystem include: 1) the input-to-output transfer function $A_u = v_o/v_s$, 2) the output impedance $Z_o = v_o/i_o$, 3) the loop gain $T_m = -F_v u_y/u_{x\,v_s=0}$ and 4) the input impedance $Z_i = v_s/i_s$. Table I shows the expressions for these performance criteria, along with definitions for the various transfer functions appearing in the performance criteria. The first term in each performance criterion is the transfer function of the dc-to-dc converter or source subsystem, and the latter fractional term represents the effects of the dynamic interaction. The four different input impedances, Z_{iC}, Z_i', Z_i'', and Z_i''', whose definitions are given in Table I, are involved in the fractional terms. Therefore, they should be analyzed prior to investigating the converter's performance under the dynamic interaction.

III. METHOD OF INPUT IMPEDANCE ANALYSIS

When standard circuit analysis techniques are applied to Fig. 1(b) for input impedance evaluation, the analysis soon becomes intractable and does not yield any suitable results for dynamic interaction studies. In this paper, two non-conventional circuit analysis techniques, Middlebrook's extra element theorem [13] and the feedback theorem [14], are combined with the Bode plot analysis method to express the input impedances in a factorized time-constant structure. The resulting expressions are converted into asymptotic Bode plots to display the characteristic features of the input impedances. The asymptotic plots of the input impedances can be used as a basis for future interaction analyses involved with dc-to-dc converters.

A. Derivation of Input Impedances

As the first analysis step, Middlebrook's extra element theorem [13] is applied to Fig. 1(b). This yields a general expression for a transfer function that relates the input current i_s' to the input voltage v_s' of the converter.

$$H(s) \equiv \frac{v_s'}{i_s'} = H_0\frac{1+F_v(s)\bar{B}}{1+F_v(s)B} \tag{1}$$

where H_0 denotes the transfer function $H(s)$ evaluated with $F_v = 0$, $H_0 = v_s'/i_{s\,F_v=0}'$, becoming an open-loop transfer function. This transfer function is referred to as the driving point impedance [14]. The transfer function B represents the gain of the forward path associated with

$F_v(s)$, $B = -u_y / u_{x\,i_s'=0}$, evaluated under the condition that the input variable of the transfer function is disabled. Finally, $\bar{B}$ is the gain of the forward path, $\bar{B} = -u_y / u_{x\,v_s'=0}$, evaluated under the condition that the output variable of the transfer function is nullified. This transfer function is called the null forward gain. Expression (1) can be rearranged into an alternative form, known as Middlebrook's feedback theorem [14].

$$H(s) = H_\infty \frac{T}{1+T} + H_0 \frac{1}{1+T} \tag{2}$$

where T represents the loop gain of the converter, $T = F_v B$, and H_∞ is the transfer function $H(s)$ evaluated with $F_v = \infty$, and $H_\infty = v_s' / i_s'\,_{F_v=\infty}$, namely under the condition that the output voltage of the converter is nullified. The four input impedances listed in Table I are determined by evaluating Equ. (1) or Equ. (2) with the four respective operational conditions: $Z_{iC} = H(s)$, $Z_i' = H(s)_{u_x=0\ Z_C=0}$, $Z_i'' = H(s)_{v_o=u_y=0}$, and $Z_i''' = H(s)_{u_x=0}$. The detailed steps of deriving the input impedances for the three basic PWM converters are provided in Tables II, IV and VI.

B. Simplification of Input Impedances

Expression (2) is also used to simplify the equations for the input impedances based on their asymptotic behavior. For example, the closed-loop input impedance Z_{iC} can be expressed as:

$$Z_{iC} = Z_{iC\infty} \frac{T}{1+T} + Z_{iC0} \frac{1}{1+T} \tag{3}$$

where $Z_{iC\infty} \equiv v_s' / i_s'\,_{F_v=\infty}$ is the input impedance evaluated with an infinite feedback gain, and $Z_{iC0} = v_s' / i_s'\,_{F_v=0}$ is the input impedance evaluated with a zero feedback gain. Therefore, $Z_{iC\infty}$ becomes the null input impedance Z_i''. Likewise, Z_{iC0} corresponds to the open-loop input impedance Z_i'''. Using these facts, expression (3) is modified to:

$$Z_{iC} = Z_i'' \frac{T}{1+T} + Z_i''' \frac{1}{1+T} \tag{4}$$

To extract the asymptotic behavior of Z_{iC}, expression (4) is now approximated to:

$$Z_{iC} = \begin{cases} Z_i'' & \text{at frequencies where } 1 << |T| \\ Z_i''' & \text{at frequencies where } 1 >> |T| \end{cases} \tag{5}$$

The above equation describes the asymptotic characteristics of the closed-loop input impedance. The closed-loop input impedance Z_{iC} follows the null input impedance Z_i'' before the $0\,\text{dB}$ crossover frequency of the loop gain. Thereafter, it tracks the open-loop impedance Z_i'''. The graphical Bode plot method [15] can be applied to Equ. (5) in order to cast the asymptotic approximation of the input impedance into a factorized time-constant structure. This analysis technique is extensively used in a nested manner throughout the analysis steps. This is done in order to simplify the complex input impedance expressions.

IV. Input Impedances of Three Basic PWM DC-To-DC Converters

Based on the analysis procedures outlined in Section III, the input impedances of the three basic PWM converters are derived in the standard time-constant form. The accuracy of the input impedance expressions is verified with both computer simulations and experimental results. The derivations and verifications of the 24 input impedances are summarized in Tables II through VII for easy referencing.

A. Input Impedances of Boost Converter

Table II shows the derivation steps and expressions for the four input impedances of the boost converter with either the voltage mode control or the current mode control. First, the output-shorted open-loop input impedance Z_i' is derived by explicitly evaluating Equ. (1). On the other hand, the open-loop input impedance Z_i''' is obtained by combining Equ. (1) and Equ. (2), and subsequently determining the transfer functions contained in the resulting Z_i''' expression. The null input impedance Z_i'' is directly determined from its definition. The closed-loop input impedance Z_{iC} is analyzed using Equ. (5) with the incorporation of the Z_i'' and Z_i''' characteristics. The input impedances are initially derived for current model control, and later reduced to simpler expressions for voltage mode control.

The outcomes of the input impedance analysis are validated using a prototype boost converter. The power stage/controller parameters and operational conditions of the prototype converter are given in Table III. The accuracy of the analysis results is verified in Table III by comparing the theoretical, simulated, and measured input impedances of the prototype converter. Theoretical Bode plots are constructed from the input impedance expressions. The simulated plots are obtained from the small-signal model of the converter in Fig. 1(b). Experimental data are obtained from the prototype converter using an HP4194A impedance analyzer.

B. Input Impedances of Buck and Buck/boost Converters

The input impedances of the buck converter are derived in a similar way to the boost converter case. The derivations and final expressions of the input impedances are shown in Table IV. Information on the prototype buck converter is

TABLE II
INPUT IMPEDANCE ANALYSIS FOR BOOST CONVERTER

Z_i'

Definition

$$Z_i' = \frac{v_s'}{i_s'}_{\substack{u_x=0 \\ Z_C\to 0}} \equiv H_o' \frac{1+\beta\bar{B}'}{1+\beta B'}$$

$$\beta = d/i_L = -R_i F_m \qquad H_o' = \frac{v_s'}{i_s'}_{\beta\to 0} = sL + R_D$$

$$\bar{B}' = -\frac{i_L}{d}_{v_s'\to 0} = \frac{V_D}{sL+R_D} \qquad B' = -\frac{i_L}{d}_{i_s'\to 0} = 0$$

Expression

Voltage mode control ($\beta = 0$)	Current mode control
$Z_i' = H_o' = R_D\left(1+\frac{s}{\omega_z'}\right)$	$Z_i' = K_C' \frac{1+s/Q'\omega_o' + s^2/\omega_o'^2}{1+s/\omega_p}$
$\omega_z' = \frac{R_D}{L}$	$K_C' = R_D - V_D R_i F_m'$
	$\omega_o' = \sqrt{K_C'\omega_p/L}$
	$Q' = \frac{K_C'}{\omega_o'(L + R_D/\omega_p)}$

Z_i''

Current mode control and voltage mode control

$$Z_i'' = \frac{v_s'}{i_s'}_{v_o=u_y=0} = -K''\left(1-\frac{s}{\omega_z''}\right)$$

$$K'' = D'^2 R_{DC} + D'(D-D')R_c - R_D \approx D'^2 R_{DC}$$

$$\omega_z'' = \frac{K''}{L}$$

Z_i'''

Definition

$$Z_i''' = \frac{v_s'}{i_s'}_{u_x=0} \equiv Z_{i\infty}''' \frac{T_i'''}{1+T_i'''} + Z_{i0}''' \frac{1}{1+T_i'''}$$

$$T_i''' = \frac{k_r F_m \frac{v_o}{d}_{i_s'=0}}{1 + R_i F_m \frac{i_L}{d}_{i_s'=0}}$$

$$Z_{i\infty}''' = \frac{v_s'}{i_s'}_{k_r\to\infty} = Z_i'' = -D'\frac{V_D}{I_L} + R_D + sL$$

$$Z_{i0}''' = \frac{v_s'}{i_s'}_{k_r\to 0} \equiv H_o''' \frac{1+\beta\bar{B}'''}{1+\beta B'''}$$

$$H_o''' = \frac{v_s'}{i_s'}_{\beta\to 0} = sL + R_D + D'^2 Z_C$$

$$\bar{B}''' = -\frac{i_L}{d}_{v_s'\to 0} = \frac{V_D + D' I_L Z_C}{sL + R_D + D'^2 Z_C}$$

$$\bar{B}''' = -\frac{i_L}{d}_{i_s'\to 0} = 0 \qquad Z_C = R_c + \frac{1}{sC}$$

Expression

Voltage mode control ($T_i''' = 0,\ \beta = 0$)

$$Z_i''' = H_o''' = \frac{D'^2}{C}\frac{1+s/Q'''\omega_o''' + s^2/Q'''\omega_o'''^2}{s}$$

$$\omega_o''' = D'\sqrt{\frac{1}{LC}} \qquad Q''' = \frac{D'^2}{\omega''' C(R_D + R_c D'^2)}$$

Current mode control

$$Z_i''' \approx Z_{i0}''' = Z_i' + \frac{K_C'''(1+s/\omega_{z1}''')(1+s/\omega_{z2}''')}{s(1+s/\omega_p)}$$

$$K_C''' = \frac{D'(D' - I_L R_i F_m')}{C} \qquad \omega_{z1}''' = \frac{1}{CR_c} \qquad \omega_{z2}''' = \frac{\omega_p C K_C'''}{D'^2}$$

Refer to Fig. 1(b) for the expressions of the parameters whose definitions are not explicitly given in the table.

given in Table V. The theoretical, simulated, and measured input impedances of the prototype converter are shown in Table V. Tables VI and VII show the analysis, validation, and verification of the input impedances of the prototype buck/boost converter. The close correlation between the analytical predictions and experimental results confirms the accuracy of the analysis.

V. APPLICATION EXAMPLE: INPUT FILTER INTERACTION IN CURRENT-MODE CONTROLLED BUCK CONVERTER

This section demonstrates an application of the main results of this paper on the dynamic analysis of a current-mode controlled buck converter coupled with an input filter in front. Previous publications [4], [5] reported that the loop gain and output impedance of the current-mode controlled buck converter are insensitive to any changes in the internal dynamics of the converter due to the dynamic interaction with the input filter. In other words, the loop gain and output impedance are essentially unaffected by the input filter that pushes the converter to the edge of the stable region or even well into the unstable region. This eccentric behavior will be clearly explained using the results of this paper.

The performance of the current-mode controlled buck converter is investigated using three different input filters, each presenting a different degree of dynamic interaction. The degree of interaction can be judged by comparing the output impedance of the input filter against the input impedances of the buck converter [6], [7]. Fig. 2(a) shows the four input impedances of the current-mode controlled buck

TABLE III
INPUT IMPEDANCE VERIFICATION FOR BOOST CONVERTER

	Voltage mode control	Current mode control
Power stage parameters and operational conditions	$V_S = 24$ V, $V_O = 46$ V, $I_O = 2$ A, $T_s = 20\mu s$, $L = 160\ \mu$H, $R_l = 45$ mΩ, $C = 400\mu F$, $R_c = 50$ mΩ	
Feedback controller	$s_e = 8.5\times10^4$ V/s $F_v(s) = \dfrac{400(1+s/1.3\times10^3)(1+s/4.5\times10^3)}{s(1+s/3.9\times10^4)(1+s/5.0\times10^4)}$	$R_i = 0.45$ $s_e = 3.9\times10^4$ V/s $F_v(s) = \dfrac{6.2\times10^3(1+s/1.65\times10^3)}{s(1+s/3.9\times10^4)}$
Theoretical Bode Plots	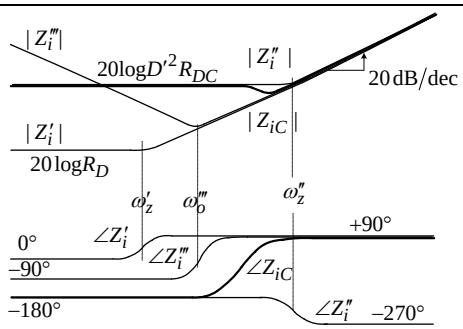	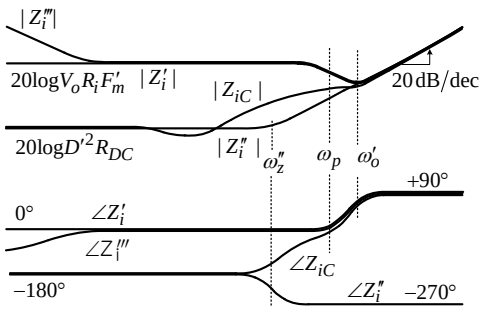
Simulated and measured Bode plots	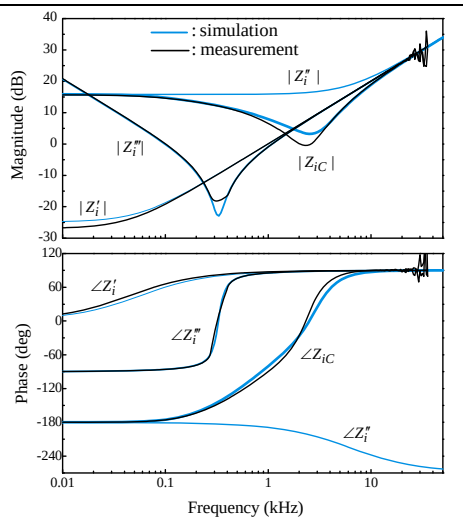	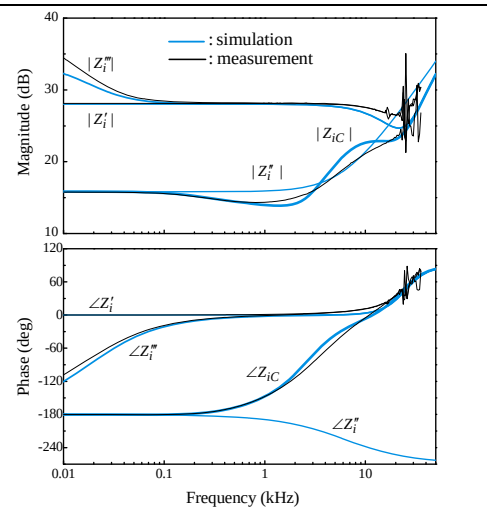

[1]The null input impedance, Z_i'', is not experimentally measurable and therefore is not included in the experimental data.

[2]The $|Z_{iC}|$ plot is drawn based on (5), which indicates $|Z_{iC}|$ follows $|Z_i''|$ before the loop gain crossover and tracks $|Z_i'''|$ thereafter.

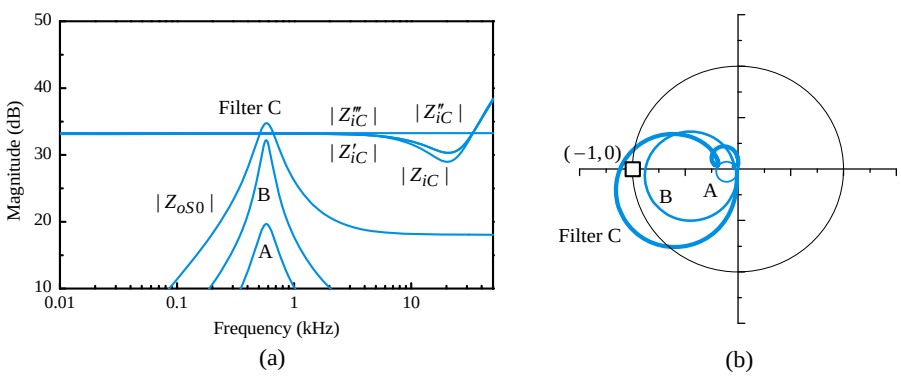

Fig. 2. Driving point impedances and output impedances of input filters. (a) Bode plot of impedances. (b) Polar plots of. Z_{oS0} / Z_{iC}.

TABLE IV
INPUT IMPEDANCE ANALYSIS FOR BUCK CONVERTER

Z_i'	Z_i'''
Definition	**Definition**
$Z_i' = \left.\frac{v_s'}{i_s'}\right\|_{\substack{u_x=0 \\ Z_C\to 0}} \equiv Z_{i\infty}' \frac{T_i'}{1+T_i'} + Z_{i0}' \frac{1}{1+T_i'}$ $T_i' = \frac{-R_i F_m \left.\frac{i_L}{d}\right\|_{i_s'=0}}{1-k_f F_m \left.\frac{v_s'}{d}\right\|_{i_s'=0}}$ $Z_{i\infty}' = \left.\frac{v_s'}{i_s'}\right\|_{R_i\to\infty} = -\frac{R_{DC}}{D^2}$ $Z_{i0}' = \left.\frac{v_s'}{i_s'}\right\|_{R_i\to 0} \equiv H_o' \frac{1+\beta\bar{B}'}{1+\beta B'}$ $\beta = \frac{d}{v_s'} = k_f F_m \quad H_o' = \left.\frac{v_s'}{i_s'}\right\|_{\beta\to 0} = \frac{sL+R_D}{D^2}$ $\bar{B}' = -\left.\frac{v_s'}{d}\right\|_{v_s'\to 0} = 0$ $B' = -\left.\frac{v_s'}{d}\right\|_{i_s'\to 0} = \frac{V_D}{D} + \frac{I_L}{D^2}(sL+R_D)$	$Z_i''' = \left.\frac{v_s'}{i_s'}\right\|_{u_x=0} \equiv Z_{i\infty}''' \frac{T_i'''}{1+T_i'''} + Z_{i0}''' \frac{1}{1+T_i'''}$ $T_i''' = -\frac{-R_i F_m \left.\frac{i_L}{d}\right\|_{i_s'=0}}{1-k_f F_m \left.\frac{v_s'}{d}\right\|_{i_s'=0}}$ $Z_{i\infty}''' = \left.\frac{v_s'}{i_s'}\right\|_{R_i\to\infty} = -\frac{V_S}{I_L D} = -\frac{R_{DC}}{D^2}$ $Z_{i0}''' = \left.\frac{v_s'}{i_s'}\right\|_{R_i\to 0} \equiv H_o''' \frac{1+\beta\bar{B}'''}{1+\beta B'''}$ $H_o''' = \left.\frac{v_s'}{i_s'}\right\|_{\beta\to 0} = \frac{sL+R_D+Z_C}{D^2}$ $\bar{B}''' = \left.\frac{v_s'}{d}\right\|_{v_s'\to 0} = 0$ $B''' = \left.\frac{v_s'}{d}\right\|_{i_s'\to 0} = \frac{V_D}{D} + \frac{I_L}{D^2}(sL+R_D+Z_C)$
Expression	**Expression**
Voltage mode control $(T_i'=0,\ \beta=0)$	Voltage mode control $(T_i'''=0,\ \beta=0)$
$Z_i' = H_o' = K_V'(1+s/\omega_z') \quad K_V' = R_D/D^2 \quad \omega_z' = R_D/L$	$Z_i''' = H_o''' = \frac{1}{D^2 C}\frac{1+s/Q'''\omega_o''' + s^2/Q'''\omega_o'''^2}{s}$ $\omega_o''' = \sqrt{\frac{1}{LC}} \qquad Q''' = \frac{1}{\omega''' C(R_D+R_c)}$
Current mode control	Current mode control
$Z_i' = K_C' \frac{1+s/Q'\omega_o' + s^2/\omega_o'^2}{1+s/\omega_p'} \quad K_C' = \frac{R'}{D^2 k_f'} \approx -\frac{R_{DC}}{D^2}$ $\omega_o' = \sqrt{\frac{R'\omega_p}{L}} \qquad Q' = \frac{R'}{\omega_o'(L+R_D/\omega_p)}$ $\omega_p' = \frac{\omega_p k_f'}{1+\omega_p k_f F_m' I_L L/D^2} \qquad R' = \frac{R_i F_m' I_L R_{DC}}{D} + R_D$ $k_f' = 1 + \frac{k_f F_m' V_D}{D} + \frac{k_f F_m' I_L R_D}{D^2} - \frac{R_i F_m' I_L}{D}$	$Z_i''' \approx Z_i'$ for all frequencies
	Z_i''
	Current mode control and voltage mode control
	$Z_i'' = \left.\frac{v_s'}{i_s'}\right\|_{v_o=u_y=0} = -\frac{R_{DC}}{D^2}$

converter. As shown in Tables IV and V, the four impedances of the converter show the same low-frequency asymptote. The output impedance, Z_{oS0}, of the three different input filters, Filter A, Filter B, and Filter C, are also shown in Fig. 2(a).

As shown in Fig. 2(a), the peak value of the filter output impedance, $|Z_{oS0}|_{peak}$, is successively increased in order to produce escalating degrees of input filter interaction. The converter remains stable when the condition $|Z_{oS0}|_{peak} < |Z_{iC}|$ is met [3]. Filter A well satisfies the stability condition and also meets the condition $|Z_{oS0}|_{peak} << |Z_{iC}|$. This ensures the stable operation of the converter and the converter performance is not affected by the input filter. Filter B barely satisfies the stability condition with $|Z_{oS0}|_{peak}$ nearing $|Z_{iC}|$. Although the converter is stable, its performance is adversely affected by the input filter. Lastly, Filter C violates the stability condition.

Polar plots of the impedance ratio of Z_{oS0}/Z_{iC} for the three filters are shown in Fig. 2(b). Filter A well satisfies the

TABLE V
INPUT IMPEDANCE VERIFICATION FOR BUCK CONVERTER

	Voltage mode control	Current mode control
Power stage parameters and operational conditions	$V_S = 46$ V, $V_O = 15$ V, $I_O = 3.067$ A, $T_s = 20$ μs, $L = 180$ μH, $R_l = 120$ mΩ, $C = 400$ μF, $R_c = 35$ mΩ	
Feedback controller	$s_e = 8.5\times10^4$ V/s, $F_v(s) = \dfrac{4\times10^3(1+s/2.36\times10^3)(1+s/6.9\times10^3)}{s(1+s/4.17\times10^4)(1+s/1.8\times10^5)}$	$R_i = 0.39$, $s_e = 1.4\times10^4$ V/s, $F_v(s) = \dfrac{1\times10^4(1+s/2.3\times10^3)}{s(1+s/6.7\times10^4)}$
Theoretical Bode Plots	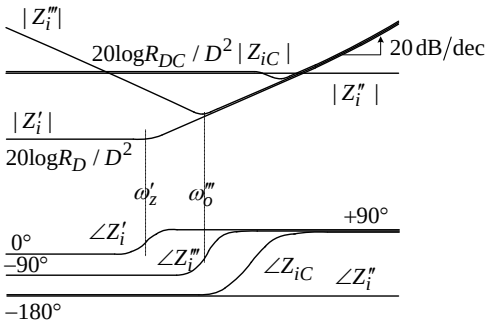	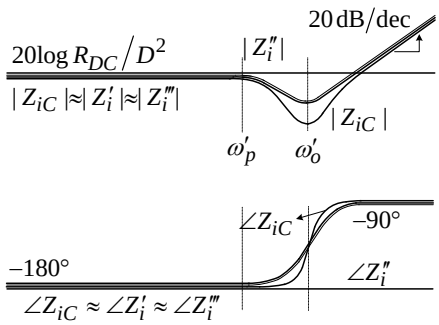
Simulated and measured Bode plots	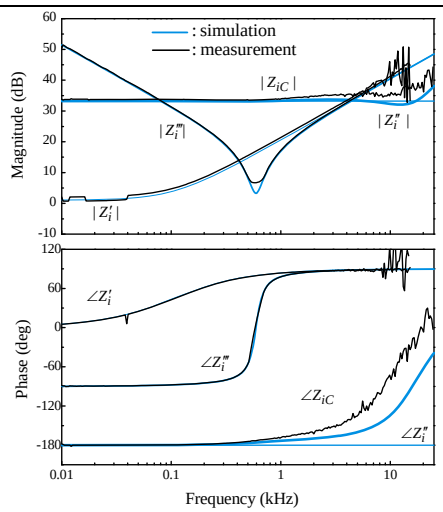	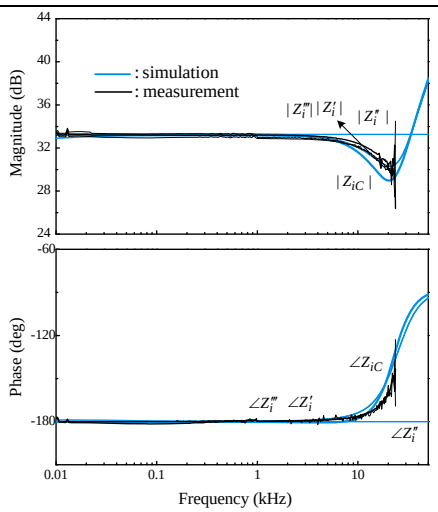

Nyquist stability criterion, while Filter B manages to meet the stability criterion with very small margin. On the other hand, Filter C encircles the (-1, 0) point, thus violating the Nyquist stability criterion.

Fig. 3 shows the output impedance, loop gain, and step load response of the buck converter coupled with the three different input filters. The output impedance of the input-filter coupled buck converter is given by:

$$Z_o(s) = Z_{oC}(s)\frac{1+Z_{oS}/Z_i'(s)}{1+Z_{oS}/Z_{iC}(s)} \tag{6}$$

The input impedance analysis in Table IV and V indicates that $Z_{iC} \approx Z_i'(s)$. Thus, the output impedance of the converter is reduced to $Z_o(s) \approx Z_{oC}(s)$. This indicates that the effects of the input filter are totally hidden and that the output impedance always stays the same, regardless of any changes in the stability and other internal dynamics of the converter. The output impedance plots in Fig. 3(a) verify this fact.

The phenomenon found in the output impedance also occurs in the loop gain in Fig. 3(b). With the prevailing condition of $Z_i''(s) \approx Z_i'''(s)$, the loop gain becomes:

$$T_m(s) = T_{mC}(s)\frac{1+Z_{oS0}/Z_i''(s)}{1+Z_{oS0}/Z_i'''(s)} \approx T_{mC}(s) \tag{7}$$

The loop gain is unaltered for all of the cases and does not show any hint of unusual behavior when the converter is at the borderline of stability or even in deep instability. This situation is the same as the output impedance case.

The step load current response of the buck converter is

TABLE VI
INPUT IMPEDANCE ANALYSIS FOR BUCK/BOOST CONVERTER

Z_i'

Definition

$$Z_i' = \left.\frac{v_s'}{i_s'}\right|_{\substack{u_x=0\\ Z_C\to 0}} \equiv Z_{i\infty}' \frac{T_i'}{1+T_i'} + Z_{i0}' \frac{1}{1+T_i'}$$

$$T_i' = \frac{-R_i F_m \left.\frac{i_L}{d}\right|_{i_s'=0}}{1 - k_f F_m \left.\frac{v_s'}{d}\right|_{i_s'=0}}$$

$$Z_{i\infty}' = \left.\frac{v_s'}{i_s'}\right|_{R_i\to\infty} = -\frac{V_D}{DI_L} = -\frac{R_{DC}D'}{D^2}$$

$$Z_{i0}' = \left.\frac{v_s'}{i_s'}\right|_{R_i\to 0} \equiv H_o' \frac{1+\beta\bar{B}'}{1+\beta B'}$$

$$\beta = d/v_s' = k_f F_m \quad H_o' = v_s'/i_{s\,\beta\to 0}' = (sL+R_D)/D^2$$

$$\bar{B}' = -v_s'/d_{\,v_s'\to 0} = 0$$

$$B' = -v_s'/d_{\,i_s'\to 0} = V_D/D + I_L(sL+R_D)/D^2$$

Expression

Voltage mode control ($T_i'=0,\ \beta=0$)	Current mode control
$Z_i' = H_o' = K_V'(1+s/\omega_z')$	$Z_i' = K_C' \dfrac{1+s/Q'\omega_o' + s^2/\omega_o'^2}{1+s/\omega_p'}$
$K_V' = \dfrac{R_D}{D^2} \quad \omega_z' = \dfrac{R_D}{L}$	$K_C' = \dfrac{V_D'}{D^2 k_f'} \approx -\dfrac{R_{DC}D'}{D^2}$
$\omega_o' = \sqrt{V_D'\omega_p/L}$	$\omega_p' = \dfrac{\omega_p k_f'}{1+\omega_p k_f F_m' I_L L/D^2}$
$Q' = V_D'/\omega_o'(L+R_D/\omega_p)$	$V_D' = R_i F_m' V_D + R_D$
	$k_f' = 1 + \dfrac{k_f F_m' V_D}{D} + \dfrac{k_f F_m' I_L R_D}{D^2} - \dfrac{R_i F_m' I_L}{D}$

Z_i''

Current mode control and voltage mode control

$$Z_i'' = \left.\frac{v_s'}{i_s'}\right|_{v_o=u_y=0} = -K''\left(1+\frac{s}{\omega_z''}\right)$$

$$K'' = \frac{1}{D}\left(\frac{D'V_D}{I_L} - R_D\right) \approx \frac{D'^2 R_{DC}}{D^2} \quad \omega_z'' = \frac{DK''}{L}$$

$$V_D''' = R_i F_m'(V_D + D' I_L Z_C) + R_D + D'^2 Z_C$$

$$k_f''' = 1 + k_f F_m'\left(\frac{V_D}{D} + \frac{I_L}{D^2}(R_D + D'Z_C)\right) - R_i F_m' \frac{I_L}{D}$$

Z_i'''

Definition

$$Z_i''' = \left.\frac{v_s'}{i_s'}\right|_{u_x=0} \equiv Z_{i\infty}''' \frac{T_i'''}{1+T_i'''} + Z_{i0}''' \frac{1}{1+T_i'''}$$

$$T_i''' = -\frac{k_r F_m \left.\frac{v_o}{d}\right|_{i_s'=0}}{1 - k_f F_m \left.\frac{v_s'}{d}\right|_{i_s'=0} + R_i F_m \left.\frac{i_L}{d}\right|_{i_s'=0}}$$

$$Z_{i\infty}''' = v_s'/i_{s\,k_r\to\infty}' = Z_i''$$

$$Z_{i0}''' = \left.\frac{v_s'}{i_s'}\right|_{k_r\to 0} \equiv Z_\infty \frac{T_0}{1+T_0} + Z_0 \frac{1}{1+T_0}$$

$$T_0 = \frac{R_i F_m \left.\frac{i_L}{d}\right|_{i_s'=0}}{1 - k_f F_m \left.\frac{v_s'}{d}\right|_{i_s'=0}}$$

$$Z_\infty = v_s'/i_{s\,R_i\to\infty}' = -\frac{V_D}{DI_L} - \frac{D'}{D} Z_C$$

$$Z_0 = v_s'/i_{s\,R_i\to 0}' = H_o''' \frac{1+\beta\bar{B}'''}{1+\beta B'''}$$

$$H_o''' = \left.\frac{v_s'}{i_s'}\right|_{\beta\to 0} = \frac{sL + R_D + D'^2 Z_C}{D^2}$$

$$\bar{B}''' = v_s'/d_{\,v_s'\to 0} = 0$$

$$B''' = v_s'/d_{\,i_s'\to 0} = \frac{V_D}{D} + \frac{I_L}{D^2}(sL + R_D + D'^2 Z_C)$$

Expression

Voltage mode control ($T_i'''=0,\ T_0=0,\ \beta=0$)

$$Z_i''' = H_o''' = K_V''' \frac{1+s/Q_v'''\omega_{vo}''' + s^2/\omega_{vo}'''^2}{s}$$

$$K_V''' = D'^2/(CD^2) \quad \omega_{vo}''' = D'\sqrt{1/LC}$$

$$Q_v''' = D'^2/(\omega_{vo}''' C(R_D + D'^2 R_c))$$

Current mode control

$$Z_i''' \approx Z_{i,0}''' = K_C''' \frac{1+s/Q'''\omega_o''' + s^2/\omega_o'''^2}{1+s/\omega_p'''}$$

$$K_C''' = \frac{V_D'''}{D^2 k_f'''} \quad Q''' = \frac{V_D'''}{\omega_o'''(L + (R_D + D'^2 Z_C)/\omega_p)}$$

$$\omega_o''' = \sqrt{\frac{V_D'''\,\omega_p}{L}} \quad \omega_p''' = \frac{\omega_p k_f'''}{1+\omega_p k_f F_m' I_L L/D^2}$$

TABLE VII
INPUT IMPEDANCE VERIFICATION FOR BUCK/BOOST CONVERTER

	Voltage mode control	Current mode control
Power stage parameters and operational conditions	$V_S = 20$ V, $V_O = 30$ V, $I_O = 1.5$ A, $T_s = 20$ μs, $L = 140$ μH, $R_l = 80$ mΩ, $C = 400$ μF, $R_c = 40$ mΩ	
Feedback controller	$s_e = 8.5\times10^4$ V/s, $F_v(s) = \dfrac{70\,(1+s/950)\,(1+s/5.0\times10^3)}{s\,(1+s/3.9\times10^4)\,(1+s/6.28\times10^4)}$	$R_i = 0.32$, $s_e = 4.7\times10^4$ V/s, $F_v(s) = \dfrac{3.7\times10^3\,(1+s/1.2\times10^3)}{s\,(1+s/3.85\times10^4)}$
Theoretical Bode Plots	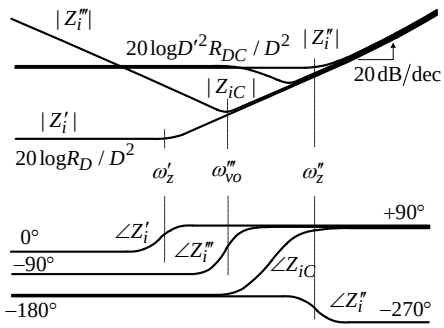	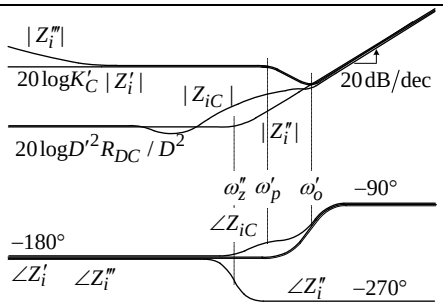
Simulated and measured Bode plots	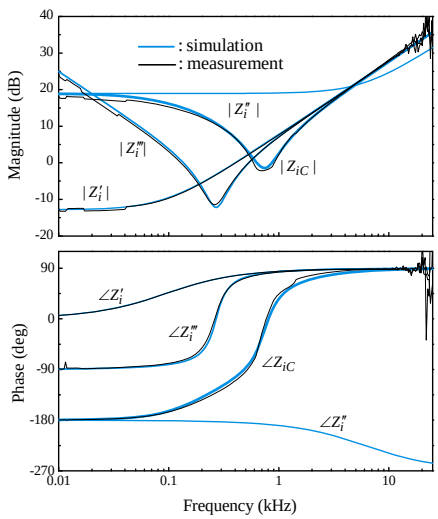	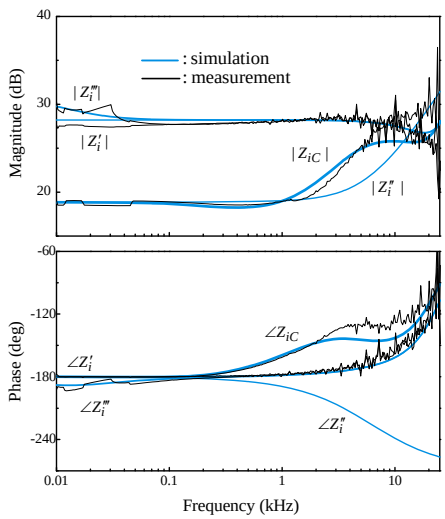

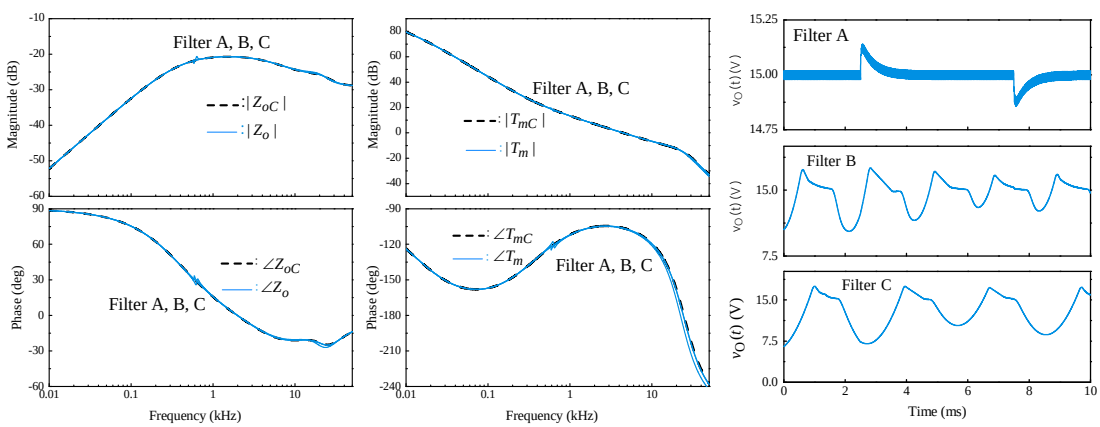

(a) (b) (c)

Fig. 3. Closed-loop performance of current-mode-controlled buck converter with input filters. (a) Output impedance. (b) Loop gain. (c) Step load response.

shown in Fig. 3(c). The output voltage in response to the load current changes is displayed in this figure. Filter A produces a very stable transient response. With Filter B, the output shows a nearly unstable response, as predicted from the small-signal analysis. The converter exhibits a full oscillation due to the instability of Filter C.

As demonstrated in this section, the peculiar behavior of the input-filter coupled current-mode controlled buck converter can be easily and clearly comprehended through knowledge about the converter input impedances.

VI. CONCLUSIONS

This paper proposed a unified analysis method for the input impedances of PWM converters, and presented the expressions and asymptotic plots of the input impedances obtained from the proposed method. Analytical expressions for the 24 input impedances, evaluated for the three basic converters with either voltage mode control or current mode control, are provided in a factorized time-constant form. The result of this study can be a useful reference for future interaction analyses requiring knowledge of a converter's input impedances.

The asymptotic plots of the 24 input impedances, shown in Tables III, V, and VII, will be a theoretical basis to investigate the dynamic interactions between the source subsystem and the converter, occurring under the following conditions.

1) The dc-to-dc converter remains in the continuous conduction mode (CCM) operation.
2) The dc-to-dc converter is only exposed to sufficiently small disturbances so that the small-signal assumption is not violated.

The use of the presented results was demonstrated through the application example, dealing with the small-signal dynamics of the input-filter coupled current-mode controlled buck converter.

ACKNOWLEDGMENT

This research was supported by the MSIP (Ministry of Science, ICT and Future Planning), Korea, under the ITRC (Information Technology Research Center) (IITP-2016-H8601-16-1002) supervised by the IITP (Institute for Information & communications Technology Promotion).

REFERENCES

[1] Riccobono and E. Santi, "Comprehensive review of stability criteria for dc power distribution systems," *IEEE Trans. Ind. Appl.*, Vol. 50, No. 5, p. 3525-3535, Sep. 2014.
[2] S. Vesti, T. Suntio, J. Oliver, R. Prieto, and J. Cobos, "Effect of control method on impedance-based interactions in a buck converter," *IEEE Trans. Power Electron.*, Vol. 28, No. 11, pp. 5311-5322, Nov. 2013.
[3] R. D. Middlebrook, "Input filter considerations in design and application of switching regulators." *IEEE-IAS Annu. Meeting*, pp. 366-382, 1976.
[4] S. Erich and W. Polivka, "Input filter design criteria for current-programmed regulators," *IEEE Trans. Power Electron.*, vol. 7, No. 1, pp. 143-151, Jan. 1992.
[5] Y. Jang and R. Erickson, "Physical origins of input filter oscillations in current programmed converters," *IEEE Trans. Power Electron.*, Vol. 7, No. 4, pp. 725-733, Oct. 1992.
[6] B. Choi, D. Kim, D. Lee, S. Choi, and J. Sun, "Analysis of input filter interactions in switching power converters," *IEEE Trans. Power Electron.*, Vol. 22, No. 2, pp. 452-460, Mar. 2007.
[7] D. Kim, B. Choi, D. Lee, and J. Sun, "Dynamics of current mode-controlled dc-to-dc converters with input filter stage," in *Proc. PESC '05*, pp. 2648-2656, Jun. 2005.
[8] M. Kazimierczuk and I. Cravens, R., "Input impedance of closed-loop PWM buck-boost dc-dc converter for CCM," in *Proc. IEEE ISCAS '95.*, Vol. 3, pp. 2047-2050, 1995,
[9] S. Kriventsov and J. Mayer, "An exact expression for the input impedance of the buck converter in continuous conduction mode," in *Proc. IEEE 32nd PESC. 2001 Annu.*, vol. 1, pp. 351-356, 2001.
[10] D. Kim, D. Son, and B. Choi, "Input impedance analysis of PWM dc-to-dc converters," in *Proc. IEEE 21st Annu. APEC '06*, pp. 1339-1346, Mar. 2006.
[11] S. K. Pidaparthy and B. Choi, "Designing control loop for PWM converters in dc-to-dc power conversion systems," in *Proc. IEEE 40th Annu. IECON 2014*, pp. 5094-5100, Oct. 2014.
[12] S. K. Pidaparthy and B. Choi,"Control design and loop gain analysis of dc-to-dc converters intended for general load subsystems," *Mathematical Problems in Engineering*, Vol. 2015, 2015.
[13] R. Middlebrook, V. Vorperian, and J. Lindal, "The n extra element theorem," *IEEE Trans. Circuits Syst. I Fundam. Theory Appl.*, Vol. 45, No. 9, pp. 919-935, Sep. 1998.
[14] V. Vorp´erian, *Fast Analytical Techniques for Electrical and Electronic Circuits*. Cambridge University Press, 2002.
[15] B. Choi, *Pulsewidth Modulated DC-to-DC Power Conversion: Circuits, Dynamics, and Control Designs*. John Wiley & Sons, 2013.
[16] R. W. Erickson and D. Maksimovic, *Fundamentals of Power Electronics*, Springer Science & Business Media, 2001.
[17] R. Middlebrook, "Modeling current-programmed buck and boost regulators," *IEEE Trans. Power Electron.*, Vol. 4, No. 1, pp. 36-52, Jan. 1989.
[18] B. Choi, J. Kim, B. Cho, S. Choi, and C. Wildrick, "Designing control loop for dc-to-dc converters loaded with unknown ac dynamics," *IEEE Trans. Ind. Electron.*, Vol. 49, No. 4, pp. 925-932, Aug. 2002.
[19] F. Tan and R. Middlebrook, "A unified model for current programmed converters," *IEEE Trans. Power Electron.*, Vol. 10, No. 4, pp. 397-408, Jul. 1995.
[20] V. Vorperian, "Simplified analysis of PWM converters using model of PWM switch continuous conduction mode," *IEEE Trans. Aerosp. Electron. Syst.*, Vol. 26, No. 3, pp. 490-496, May 1990.

Syam Kumar Pidaparthy received his B.Tech. degree in Electrical and Electronics Engineering from Acharya Nagarjuna University, Guntur, India, in 2010; and his M.S. degree in Circuits and Embedded Systems Engineering from Kyungpook National University (KNU), Taegu, Korea, in 2013, where he is presently working towards his Ph.D. degree. His current research interests include the modeling, dynamic analysis and control design of large-scale dc-to-dc power conversion systems.

Byungcho Choi (S'90-M'91) received his B.S. degree in Electronics from Hanyang University, Seoul, Korea, in 1980; and his M.S. and Ph.D. degrees in Electrical Engineering from the Virginia Polytechnic Institute and State University, Blacksburg, VA, USA, in 1988 and 1992, respectively. In 1996, he joined the School of Electrical Engineering and Computer Science, Kyungpook National University, Taegu, Korea, where he is presently working as a Professor. His current research interests include the modeling and design optimization of high-frequency power converters for portable electronics, computer power systems, and distributed power systems. He is the author of the book, "*Pulsewidth Modulated Dc-to-Dc Power Conversion*," New Jersey, Wiley-IEEE Press, 2013.